

# Thermal, Crystalline, and Mechanical Properties of Octa(3-chloropropylsilsesquioxane)/Poly(L-lactic acid) Hybrid Films

Xiaojing Zhang, Jiashu Sun, Shaoming Fang, Xiniu Han, Yadong Li, Chenggui Zhang

College of Materials and Chemical Engineering, Zhengzhou University of Light Industry, Henan Provincial Key Laboratory of Surface and Interface Science, Zhengzhou 450002, Henan, China

Received 13 June 2010; accepted 27 December 2010

DOI 10.1002/app.34059

Published online 21 April 2011 in Wiley Online Library (wileyonlinelibrary.com).

**ABSTRACT:** A series of organic-inorganic hybrid films were prepared based on octa(3-chloropropylsilsesquioxane) (OCPS) and poly(L-lactic acid) (PLLA) via simply solution blending method. The thermal, crystalline and mechanical properties of OCPS/PLLA hybrid films were characterized by Fourier transform infrared, scanning electron microscopy, energy dispersive spectrometer, differential scanning calorimetry (DSC), X-ray diffraction, polarized optical microscopy, thermogravimetric analysis (TGA), and tensile tests. The results showed that OCPS could be dispersed well at molecular level when its content was less than 3 wt % and began to crystallize in PLLA matrix when the content increased to 5 wt %. DSC study revealed that OCPS acted as a plasticizer to decrease both  $T_g$  and  $T_m$  of the PLLA matrix at various heating rates. The addition of OCPS did not change the crystal

form of PLLA, while had an great influence on the cold crystallization and melting behaviors of PLLA in the second heating cycles. Moreover, the initial crystallinity of OCPS/PLLA was higher than that of pure PLLA. The results suggested that OCPS could be an effective heterogeneous nucleating reagent to promote the crystallization of PLLA. TGA showed that the PLLA thermal degradation mechanism remained unchanged, whereas the weight loss temperatures and residual weights were improved. Tensile tests indicated that the incorporation of OCPS into PLLA matrix changed the tensile behavior of the hybrid films from brittle to ductile, and the strain at break was improved remarkably as a result of the plasticizer effect of OCPS. © 2011 Wiley Periodicals, Inc. *J Appl Polym Sci* 122: 296–303, 2011

**Key words:** POSS; PLLA; blends; composites

## INTRODUCTION

Organic-inorganic nanocomposite materials have been paid on considerable attention as a new class of advanced materials because of the combined advantages of the inorganic and organic components. Inorganic nanofillers such as clay, carbon nanotubes and silsesquioxanes are usually incorporated into polymer matrix to prepare hybrid materials with excellent properties.<sup>1–4</sup> Polyhedral oligomeric silsesquioxanes (POSS), is regarded as the smallest organosilica molecule, which consists of silicon-oxygen skeleton. A typical POSS molecule with the structure of octahedral-cube nanosized cage structures represented by the formula ( $R_8Si_8O_{12}$ ) has

an inorganic silica-like core ( $Si_8O_{12}$ ) surrounded by eight organic corner groups R. One or more of the organic groups can be reactive or polymerizable, which endows the POSS molecule with higher reactivity and solubility in organic solvent.<sup>5–7</sup> POSS may be incorporated into a polymer matrix in two primary ways: chemically tethered to the polymer backbone or physically blended with the polymer matrix as untethered filler particles. The properties of hybrid polymers such as thermal stability usually have been enhanced when POSS was covalently tethered to a polymer backbone.<sup>8–13</sup> However, the preparation of POSS-polymers needed to be elaborately designed and resulted in high cost. The physical blending method is simple to use and fit to prepare materials on the large scale, which can be done either via a solution route or by melt mixing. The final properties of the hybrid materials depend on the substituent and concentration of the POSS compound.<sup>14</sup>

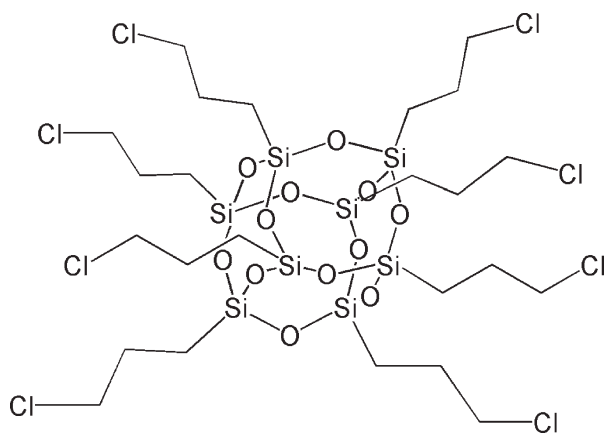
Poly(L-lactic acid) (PLLA) is a well-known biodegradable and biocompatible thermoplastic polymer.<sup>15</sup> Because of its good compatibility, favorable biodegradability, versatile fabrication processes, as well as nontoxic to the human body and the environment, PLLA has a wide variety of applications in medical devices and environmentally friendly

Correspondence to: X. Zhang (zhangxj@iccas.ac.cn).

Contract grant sponsor: The National Natural Science Foundation of China; contract grant number: 20804041.

Contract grant sponsor: Program for Innovative Research Team (in Science and Technology) in University of Henan Province; contract grant number: 2008IRTSTHN004.

Contract grant sponsor: The education department foundation of Henan Province; contract grant number: 2009A430025.



**Scheme 1** The structure of OCPS

packaging materials.<sup>16,17</sup> However, the poor thermal stability, the brittle behavior, and uncontrolled degradation rate of PLLA have limited its development and wide practical application. Incorporation of inorganic nanofiller into PLLA matrix to prepare hybrid nanocomposites is a widely used method to overcome the problems. Compared to other nanofiller/PLLA hybrid materials, reports about the preparation and properties of POSS/PLLA hybrid materials are very limited.<sup>18–20</sup> Dubois<sup>18</sup> and Jeong<sup>19</sup> both reported the preparation of POSS/PLLA copolymers via the ring-opening polymerization of L-lactide with POSS bearing one hydroxyl group. Compared with the neat PLLA, the thermal and thermooxidative degradation properties of the POSS/PLLA nanocomposites were found to be improved. The crystallization rates and crystallinities of the PLLA/POSS-PLLA nanocomposites were faster and higher, respectively, with increasing POSS-PLLA content because of the nucleation effect of the POSS molecules in the neat PLLA matrix. Among the several modifications, physical blending method is regarded as a simple and useful to prepare a large number of hybrid materials. Zhang and coworkers<sup>20</sup> prepared PLLA/PBSA/POSS composites with two types of POSS by melting blend method and investigated the morphology, rheological behavior, and thermal stability of the hybrid materials. The results showed that POSS could act as nucleating agents for PLLA and improve the thermal stability of the composites, whereas the dispersion state and the effect of POSS on the modulus and viscosity of the composites would depend on the type of the POSS.

In this work, octa(3-chloropropylsilsesquioxane) (OCPS) with eight chloropropyl groups has good solubility in ordinary solvents (Scheme 1), which can be easily incorporated into PLLA matrix by solution blending method with varying the OCPS content from 0–15 wt %. The thermal, crystalline, and mechanical properties of the resulted OCPS/PLLA

hybrid films were investigated by Fourier transform infrared (FTIR), scanning electron microscopy (SEM), energy dispersive spectrometer (EDS), differential scanning calorimetry (DSC), X-ray diffraction (XRD), polarized optical microscopy (POM), thermogravimetric analysis (TGA), and tensile tests.

## EXPERIMENTAL

### Materials

3-chloropropyltrimethoxysilane [ $\text{ClC}_3\text{H}_6\text{Si}(\text{OCH}_3)_3$ , 98%] was purchased from Nanjing Xiangfei Chemical Research Institute (China) and was used as received. Poly(L-lactic acid) (PLLA) was purchased from Shenzhen Bright China Industrial (China) with the viscosity average molecular weight  $M_v = 1.0 \times 10^5$ . Tetrahydrofuran (THF) was obtained from Tianjin Reagent (China).

### Synthesis of OCPS

OCPS was synthesized according to the procedures described in References.<sup>21,22</sup> Typically, 3-chloropropyltrimethoxysilane (79.5 g, 0.4 mol) was dissolved in 1800 mL methanol with stirring at room temperature in a round-bottomed flask, and then 90 mL concentrated hydrochloric acid was added. The system was allowed to carry out for at least 5 weeks. The white crystalline powder was filtered, washed with methanol to give 14.0 g white crystal powder, (yield: 31%), and the white crystals were obtained after dried in vacuum. The characterization data are as follows: FTIR (KBr,  $\text{cm}^{-1}$ ): 2955, 1110, 697  $\text{cm}^{-1}$ ;  $^1\text{H-NMR}$  (400 MHz,  $\text{CDCl}_3$ ):  $\delta$  3.54 (t,  $\text{CH}_2\text{Cl}$ , 16 H), 1.88 (m,  $\text{CCH}_2\text{C}$ , 16 H), 0.81 (m,  $\text{SiCH}_2$ , 16 H);  $^{29}\text{Si-NMR}$  (71.5 MHz,  $\text{CDCl}_3$ ):  $\delta$  -68.5 (s).

### Preparation of OCPS/PLLA hybrid films

A series of OCPS/PLLA hybrid films were prepared via solution blending method. Briefly, the pure PLLA (3 g) was added into THF (81 mL) and was stirred at 60°C using a magnetic stirrer, then various contents (3, 5, 10, 15 wt %) of OCPS was added into the solution, respectively. The mixture was stirred for 2 h and placed for 24 h to eliminate the bubbles. Then the solution was cast onto the neat glass plates and kept into a homemade mantle for 24 h to evaporate the solvent at room temperature. The obtained film was subsequently dried in vacuum oven at 50°C for 24 h. The pure PLLA used as a standard was treated in the same way. The compositions of the prepared OCPS/PLLA hybrid films are shown in Table I.

### Characterization

FTIR spectra were measured with a Bruker FTIR spectrophotometer (Tensor27, USA) using thin film

**TABLE I**  
The Compositions of the Prepared  
OCPS/PLLA Hybrid Films

Samples	PLLA (wt %)	OCPS (wt %)
PLLA	100	0
3%OCPS/PLLA	97	3
5%OCPS/PLLA	95	5
10%OCPS/PLLA	90	10
15%OCPS/PLLA	85	15

method on KBr disks at room temperature. The scan range was from 4000 to 500  $\text{cm}^{-1}$  with a resolution of 4  $\text{cm}^{-1}$ .

The morphology of the specimens was observed by SEM using the JSM-6490LV apparatus. The specimens were previously coated with a conductive layer of gold. The amount of Si retained by the various OCPS/PLLA samples was measured by an energy dispersive X-ray spectrometer system attached to the SEM.

Thermal analysis was performed using a TA Instruments DSC Q100 with a Universal Analysis 2000. All operations were performed under nitrogen purge, and the weight of the samples varied between 4 and 6 mg. The sample was heated from 30 to 200°C at a heating rate of 10°C/min (first heating), held for 10 min to erase the previous thermal history, cooled to 30°C at a cooling rate of 10°C/min (first cooling), and then heated to 190°C again at various heating rates of 10, 5, 2, and 1°C/min (second heating) to study the subsequent melting behavior.

Thermogravimetric analysis (TGA) was carried out using a Netzsch STA-409PC thermal analyzer. Samples weighting about 5 mg, and measurements were performed from 25°C to 600°C at a heating rate of 10°C/min under nitrogen atmosphere.

XRD was recorded with a Bruker D8 ADVANCE X-ray diffraction apparatus. The sample was scanned from 5 to 60° at a speed of 2°/min at room temperature with  $\text{CuK}\alpha$  radiation at a generator voltage of 40 V and a current of 100 mA.

Crystallization morphology was observed with a polarized optical microscope of Nikon ECLIPSE E600 with a hot stage. The samples were heated to melted at 180°C for 5 min and then rapidly cooled to 110°C for 12 h isothermal crystallization.

The tensile tests were carried out in a universal mechanical testing machine CMT-6104 controlled by video-extensometer at an extension rate of 10 mm/min and room temperature. Tensile dog-bone-shaped samples were obtained after die-cutting the compression molded films. Stress-strain curves were plotted. At least six specimens of each sample were tested, and then averaged results and standard deviations were reported.

## RESULTS AND DISCUSSION

### Preparation and FTIR analysis of OCPS/PLLA hybrid films

OCPS was prepared by the controlled hydrolysis and condensation reactions of 3-chloropropyltrimethoxysilane in methanol using concentrated hydrochloric acid as the catalyst. The eight chloropropyl groups on the cage corners would help OCPS dissolve well in ordinary solvents, such as THF, chloroform and toluene, etc. OCPS could be easily incorporated into PLLA matrix via solution blending method at a concentration of 0–15 wt %. The obtained OCPS/PLLA hybrid materials showed good film-forming properties and a series of hybrid films were prepared to study the effect of OCPS on the properties of PLLA.

The FTIR spectra of OCPS, PLLA, and OCPS/PLLA hybrid films were shown in Figure 1. A strong and sharp peak appeared at 1110  $\text{cm}^{-1}$  could be attributed to Si—O—Si asymmetric stretching vibration in OCPS, which is the typical absorption of the cage structure of POSS. Another characteristic band appeared at 697  $\text{cm}^{-1}$  for OCPS, is assigned to the stretching vibration of C—Cl. The pure PLLA showed characteristic absorption at 1758  $\text{cm}^{-1}$ , which is attributable to the stretching vibration band of the carbonyl group of the polyester. Most of the absorption peaks of OCPS and PLLA are overlapped, and the FTIR spectra of OCPS/PLLA hybrid films are very similar with that of pure PLLA, whereas the absorption peak of C—Cl in OCPS at 697  $\text{cm}^{-1}$  could be observed in the IR spectra of OCPS/PLLA and the intensity of this characteristic band increased with increasing the OCPS content.

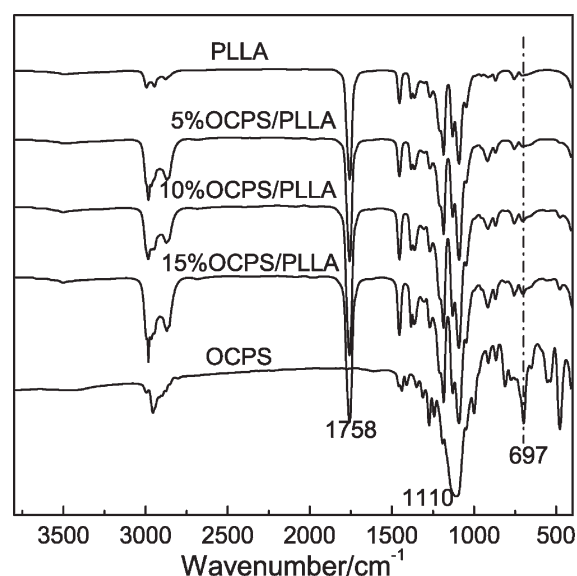


**Figure 1** FTIR spectra of OCPS, PLLA, and OCPS/PLLA hybrid films.

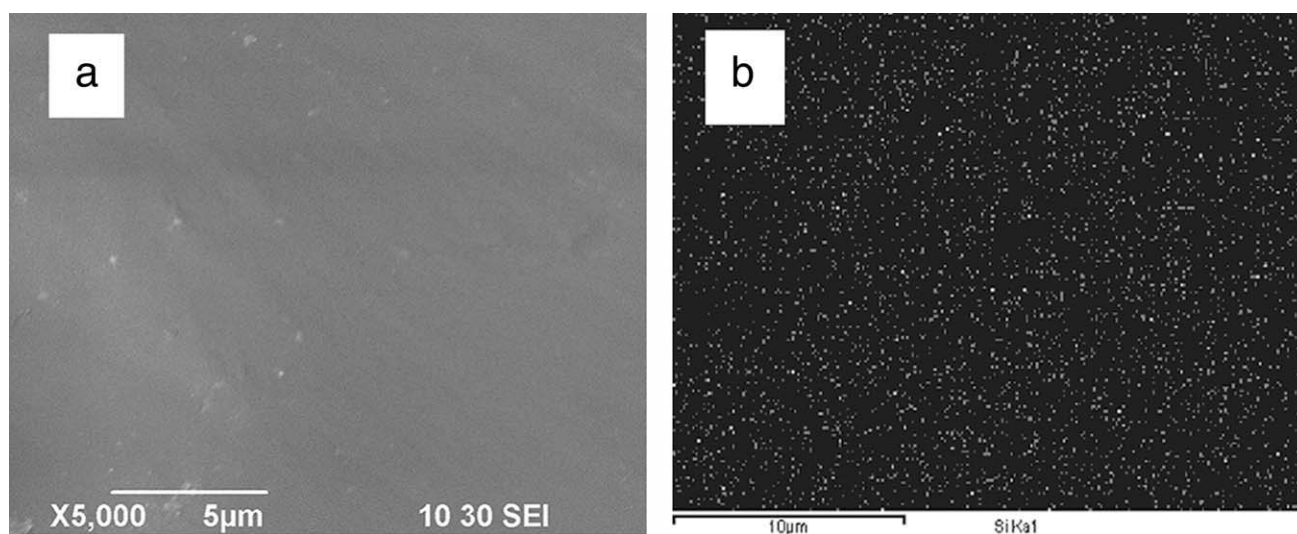


**Figure 2** SEM photograph (a) and X-ray silicon mapping (b) of 10% OCPS/PLLA hybrid film.

### Morphology and dispersion of OCPS in PLLA matrix

It is well known that the dispersion of POSS cubes in the polymer matrix plays an important role of influencing the physical properties of polymers. The morphology and dispersion state of OCPS in PLLA matrix were investigated by SEM, EDS, and XRD. Figure 2(a) shows the SEM image of 10% OCPS/PLLA hybrid film. It was found that the cross section of OCPS/PLLA hybrid films was almost smooth and homogenous except for some small particles. EDS result of OCPS/PLLA composites in Figure 2(b) reveals the dispersion state of silicon element within the polymer matrix. The white spots in the dark background indicate the location of silicon element within the hybrid composites, which can reflect the dispersion of POSS because only OCPS possesses silicon element in the hybrids. As shown in Figure 2(b), the distribution of silicon element was almost uniform, which suggested that OCPS seemed to be dispersed well in PLLA matrix till its content is up to 10 wt %. Although more details in the dispersion of OCPS could be obtained by XRD measurements, as shown in Figure 5. No typical crystalline peaks of OCPS were observed in OCPS/PLLA hybrid materials until the OCPS content is up to 5 wt %. The result indicated that OCPS could be dispersed well at molecule level at a very small loading (less than 3 wt %) and began to crystallize in PLLA matrix when its content increased to 5 wt %. So the appearance of the small particles in SEM may be due to the crystallization of OCPS in PLLA matrix.

### DSC and TGA analysis

The PLLA and OCPS/PLLA hybrid films were subjected to thermal analysis by DSC and TGA meth-

ods. No crystallization peak was found in the cooling cycle for both PLLA and OCPS/PLLA, whereas the DSC curves of PLLA and OCPS/PLLA had a significant difference in the second heating cycle. The DSC thermograms and data of the pure PLLA and OCPS/PLLA hybrid films with different content at various heating rates in the second cycle are showed in Figure 3 and Table II. For OCPS/PLLA hybrid materials, all the DSC curves displayed a single glass transition temperature ( $T_g$ ) in the experimental temperature range, and showed slightly lower  $T_g$ s than that of pure PLLA. Compared with the change in  $T_g$ , more obvious decrease in the melting temperature ( $T_m$ ) was found in OCPS/PLLA hybrid materials. For example,  $T_m$  decreased from 148.7°C, 154.4°C to 141.8°C, 152.9°C at 1°C/min heating rate when only 3 wt % OCPS was incorporated into the PLLA matrix [(Fig. 3(d), Table II)]. The results indicated the addition of OCPS would decrease both  $T_g$  and  $T_m$  of the PLLA matrix. Unlike the POSS-containing copolymers, without the restriction of the covalent bonds between POSS and polymer chain, the nanocage of POSS served as a plasticizer to increase the free volume between polymer chains. On the other hand, in case of OCPS, the flexible methylene groups around the rigid core would also have a plasticizer effect on PLLA matrix to decrease  $T_g$  and  $T_m$ . The DSC thermograms of PLLA and OCPS/PLLA also had been affected greatly by the heating rates, as shown in Figure 3. The DSC curves of PLLA only showed a single glass transition at high heating rates (10°C/min, 5°C/min), and no cold crystallization peak and melting peak were observed until the heating rates became low (2°C/min, 1°C/min). The values of both  $T_g$  and  $T_m$  also decreased with an decrease in heating rates as expected. Obviously, OCPS had a significant

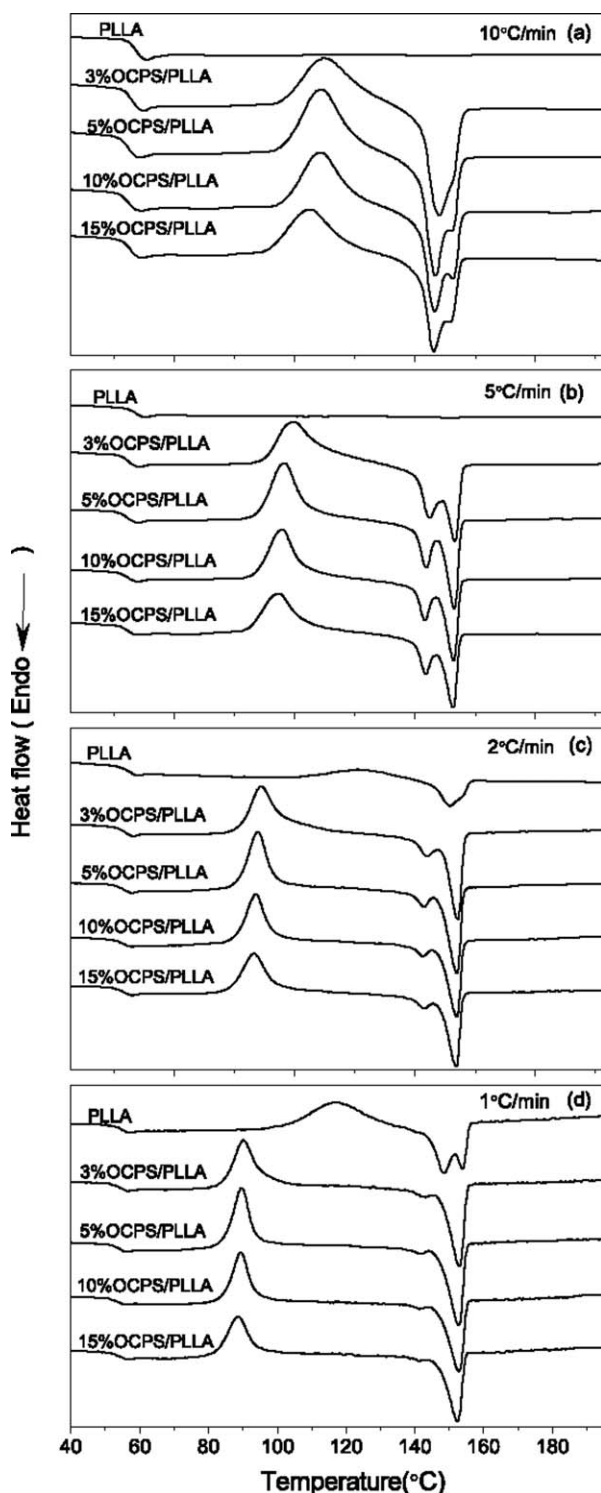


**Figure 3** DSC curves for PLLA and OCPS/PLLA hybrid films at different heating rates.

influence on the crystallization of PLLA matrix, which would be discussed carefully later.

TGA was used to evaluate the thermal stability of OCPS, PLLA, and OCPS/PLLA hybrid materials under  $N_2$  atmosphere, as shown in Figure 4 and Table III. Like most organic polymers, PLLA decom-

posed completely at less than  $600^\circ\text{C}$  as expected. On the other hand, OCPS showed good thermal stability, which resulted from the character of the inorganic materials. Its 5% weight loss temperature was slightly higher than that of PLLA, whereas the ceramic yield was still 24.4% when the PLLA decomposed completely. OCPS/PLLA hybrid materials displayed similar degradation profiles with that of pure PLLA, suggesting that OCPS component did not significantly alter the degradation mechanism of the matrix polymers. In a comparison of the thermal stabilities, weight loss temperatures at 5, 50, and 80% were enhanced for OCPS/PLLA hybrid materials after the addition of OCPS. In addition, the ceramic yields of OCPS/PLLA hybrid materials in  $580^\circ\text{C}$  also increased with increasing OCPS content. On the basis of the above analysis, it was confirmed that the thermal stability of OCPS/PLLA hybrid materials was improved by the incorporation of the OCPS inorganic component.

### Crystallization properties

The crystallization behaviors of OCPS/PLLA hybrid materials were studied by DSC, XRD, and POM methods. The cold crystallization temperatures ( $T_c$ ), melting temperatures ( $T_{m1}$  and  $T_{m2}$ ) and initial crystallinity ( $X_c$ ) of PLLA and OCPS/PLLA could be obtained from the DSC curves (Fig. 3) in the second heating scan at various heating rates and the data were listed in Table II. The pure PLLA only showed a glass transition and no cold crystallization and melting peak were observed until the heating rates decreased from 10 and  $5^\circ\text{C}/\text{min}$  to 2 and  $1^\circ\text{C}/\text{min}$ . This result indicated that the crystallization capability of PLLA used in this article is not as good as other commercially products. Different from the neat PLLA, OCPS/PLLA exhibited cold crystallization and double melting peaks at all the heating rates.  $T_c$ s of the hybrid materials decreased when increasing the OCPS content, which suggested OCPS appeared as a heterogeneous nucleating agent in PLLA matrix. The appearance of the double melting peaks revealed that the melting and recrystallization process of imperfect crystal grains. Moreover, The initial crystallinity ( $X_c$ ) was calculated from the DSC data obtained at the reheating rates of 2 and  $1^\circ\text{C}/\text{min}$  using the equation<sup>23,24</sup>:

$$X_c(\%) = \frac{\Delta H_m - \Delta H_{cc}}{X_{\text{PLLA}} \Delta H_m^0} \times 100 \quad (1)$$

where  $\Delta H_m$  is the enthalpy of fusion,  $\Delta H_{cc}$  is the cold crystallization enthalpy of PLLA during the second heating cycle,  $X_{\text{PLLA}}$  is the PLLA weight percentage in the composite.  $\Delta H_m^0$  is the enthalpy of melting of 100% crystalline PLLA, which is  $93.6 \text{ J/g}$

TABLE II  
DSC Data of PLLA and OCPS/PLLA Hybrid Films

Heating rate (°C/min)	Samples	$T_g$ (°C)	$T_c$ (°C)	$\Delta H_{cc}$ (J/g)	$T_{m1}$ (°C)	$T_{m2}$ (°C)	$\Delta H_m$ (J/g)	$X_c$ (%)
10	PLLA	56.4	/	/	/	/	/	/
	3%OCPS/PLLA	55.7	113.1	18.2	147.0	151.4	26.5	/
	5%OCPS/PLLA	53.9	113.0	23.2	146.0	151.4	25.9	/
	10%OCPS/PLLA	54.1	112.7	20.9	145.7	151.4	24.4	/
	15%OCPS/PLLA	54.5	109.9	20.7	145.4	150.8	21.8	/
5	PLLA	55.9	/	/	/	/	/	/
	3%OCPS/PLLA	54.5	104.8	28.7	144.4	151.6	30.4	/
	5%OCPS/PLLA	53.8	102.2	28.9	143.4	151.5	25.8	/
	10%OCPS/PLLA	53.9	101.5	27.3	143.0	151.3	25.1	/
	15%OCPS/PLLA	54.2	100.4	25.7	143.2	151.1	23.9	/
2	PLLA	54.2	123.6	8.6	150.2	154.0	8.9	0.32
	3%OCPS/PLLA	53.1	95.3	29.0	143.3	152.5	29.7	0.77
	5%OCPS/PLLA	52.4	94.3	24.8	142.5	152.3	25.8	1.12
	10%OCPS/PLLA	52.4	93.8	23.6	142.2	152.2	25.2	1.90
	15%OCPS/PLLA	52.9	93.1	22.6	142.5	152.0	24.4	2.26
1	PLLA	52.4	118.6	27.2	148.7	154.4	28.8	1.71
	3%OCPS/PLLA	52.1	90.0	25.4	141.8	152.9	29.7	4.74
	5%OCPS/PLLA	51.9	89.6	24.6	141.6	152.7	27.7	3.49
	10%OCPS/PLLA	51.2	89.3	22.7	141.4	152.7	25.8	3.44
	15%OCPS/PLLA	51.2	88.4	21.8	141.2	152.3	24.0	2.41

given by Fischer et al.<sup>25</sup> The results showed that  $X_c$  of OCPS/PLLA were higher than those of pure PLLA at both heating rates. So we can conclude that OCPS served as the heterogenous nucleating agent to promote the nucleation and crystallization of PLLA.

XRD measurements was used to further investigate the crystalline structure of OCPS/PLLA hybrid materials. The diffraction patterns of OCPS, PLLA, and OCPS/PLLA hybrid materials were illustrated in Figure 5. It can be observed that the OCPS is a highly crystalline material and had a characteristic dominant diffraction peak near  $12.1^\circ$  ( $2\theta$ ). The neat PLLA diffraction pattern also showed two main characteristic peaks at  $2\theta_1 \approx 16.9^\circ$  and  $2\theta_2 \approx 19.4^\circ$ , which is the typical structure of  $\alpha$ -form crystal of PLLA. For OCPS/PLLA hybrid materials, the dif-

fraction peaks at  $2\theta_1 \approx 16.9^\circ$  and  $2\theta_2 \approx 19.4^\circ$  remained unchanged compared with the neat PLLA. This suggests that the addition of OCPS does not change the crystalline structure of PLLA. Furthermore, as mentioned above, OCPS could be dispersed well at molecular level with its content less than 3 wt %, proved by the fact that the absence of characteristic peaks of OCPS in the diffraction pattern of 3% OCPS/PLLA. While a peak corresponding to the dominant OCPS crystal at  $2\theta \approx 12.1^\circ$  grew progressively in OCPS/PLLA diffraction patterns when increasing OCPS content up to 5 wt %, which indicated that OCPS could crystallize when it is dispersed physically in PLLA matrix with no chemical linkages to restrict its movement. Similar phenomenon was also observed in PMMA-POSS blend and the aggregated POSS cluster was considered to result in a  $T_g$  decrease.<sup>26</sup>  $X_c$  of PLLA and OCPS/PLLA could be calculated by software MDI Jade 5.0. The result showed that  $X_c$  of all the OCPS/PLLA was higher than that of the pure PLLA, which is in accordance with the conclusion of DSC study.

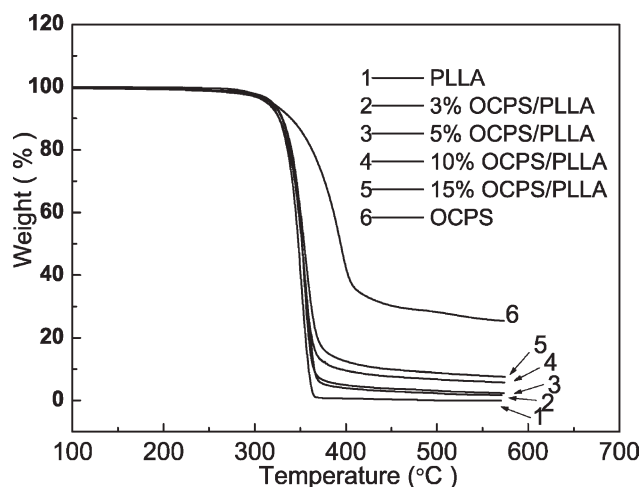
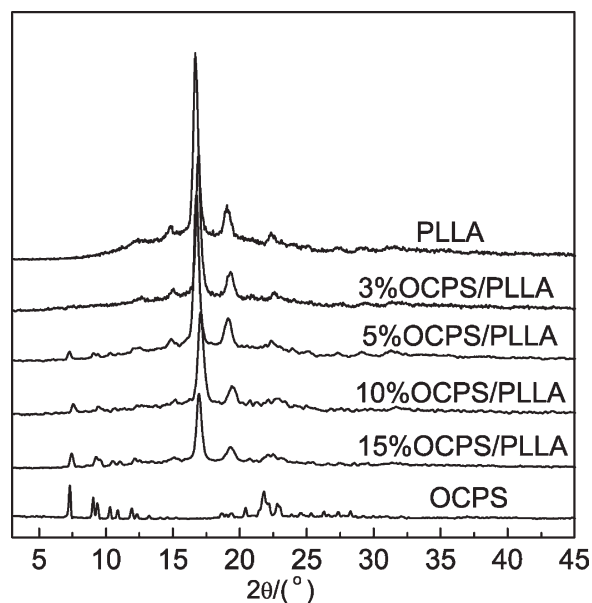


Figure 4 TGA curves of OCPS, PLLA, and OCPS/PLLA.

TABLE III  
Related Data of OCPS, PLLA and OCPS/PLLA Samples for TGA

Samples	Weight loss (°C)			Ceramic yield (%)
	5%	50%	80%	
PLLA	317	348	356	0
3%OCPS/PLLA	314	352	360	1.7
5%OCPS/PLLA	319	352	360	2.3
10%OCPS/PLLA	320	352	363	5.7
15%OCPS/PLLA	319	354	369	7.6
OCPS	319	394	/	24.4



**Figure 5** XRD patterns of OCPS, PLLA, and OCPS/PLL hybrid materials.

The morphology of PLLA and OCPS/PLL after 12 h isothermal crystallization at 110°C was observed by POM, as shown in Figure 6. It can be seen that the pure PLLA showed typical spherulite morphology, while this morphology was remarkably changed after the addition of OCPS. The nucleation density of PLLA spherulite increased with increasing OCPS content, and the size of the spherulite became very small and the boundary was unclear. The results further proved that OCPS served as a heterogeneous nucleating agent in PLLA matrix. Similar phenomenon was also observed in the isotactic polypropylene/POSS hybrid system, in which the major

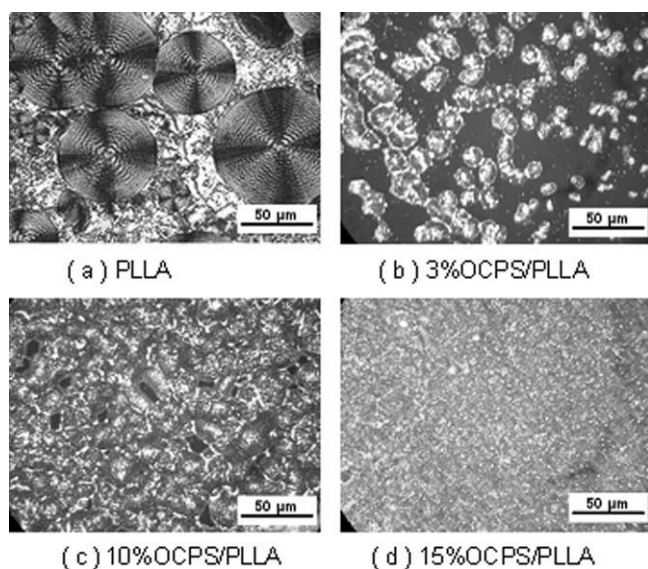


**Figure 6** Polarized optical microscopy images for PLLA and OCPS/PLL hybrid materials.

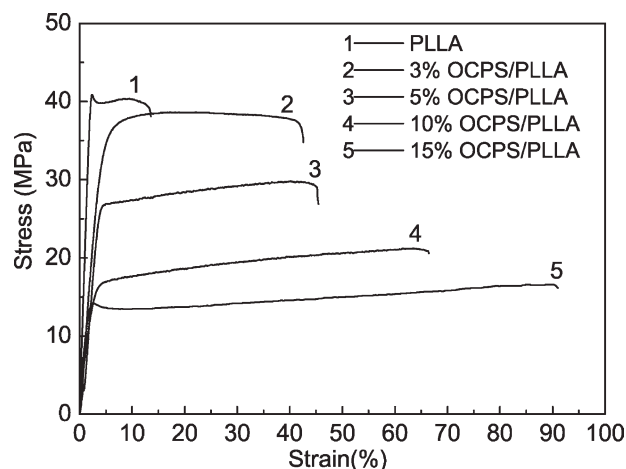


**Figure 7** Typical stress-strain curves of PLLA and OCPS/PLL hybrid films.

POSS nanocrystals appeared as an effective nucleating agent and promoted the nucleation rate of iPP.<sup>27</sup>

### Mechanical testing

The typical stress-strain curves of the different samples of PLLA and OCPS/PLL hybrid materials at an extension rate of 10 mm/min under room temperature were shown in Figure 7, and the corresponding data were summarized in Table IV. It can be observed that a well-defined yield point in pure PLLA from Figure 7, however, there was no sign of yield point after reaching the maximum stress for OCPS/PLL hybrid films. The pure PLLA exhibited brittle behavior in tensile testing and the yield strain was less than 14%, but the yield strain of OCPS/PLL hybrid films increased from 45.7 to 91.0% as the OCPS content increased from 5 to 15 wt %. The PLLA tensile behavior was changed from brittle to ductile by the incorporation of OCPS into PLLA matrix, and the strain at break was improved greatly as the results of the plasticizer effects that POSS cages take on to increase the free volume of the PLLA matrix.<sup>28</sup>

### CONCLUSIONS

Hybrid films of OCPS/PLL with varying OCPS content from 0 to 15 wt % were prepared via solution blending method. The results showed that OCPS could be dispersed well at molecule level at a very small loading (less than 3 wt %) and began to crystallize in PLLA matrix when its content increased to 5 wt %. OCPS acted as a plasticizer to decrease both  $T_g$  and  $T_m$  of the PLLA matrix at various heating rates. Although the crystal form of OCPS/PLL remained same with that of the pure PLLA, the cold crystallization and melting behaviors

**TABLE IV**  
**Related Data to Mechanical Properties of PLLA and OCPS/PLLA Hybrid Materials**

$w(\text{OCPS})/\%$	0	3	5	10	15
Tensile strength/MPa	40.9 ± 1.8	38.0 ± 1.5	28.0 ± 1.1	21.0 ± 0.9	16.1 ± 0.7
Elongation/%	13.5 ± 0.6	38.2 ± 0.9	45.7 ± 1.1	66.5 ± 1.8	91.0 ± 2.3

of PLLA in the second heating cycles were greatly changed by the addition of OCPS. At high heating rates (10°C/min, 5°C/min), the pure PLLA only showed the glass transition, whereas the cold crystallization and melting peaks could be clearly observed in OCPS/PLLA. At low heating rates (2°C/min, 1°C/min), the cold crystallization and melting peaks appeared in the pure PLLA, whereas the cold crystallization peaks were broader and  $T_c$ s shifted to lower temperatures for OCPS/PLLA. The results indicated that OCPS could be an effective heterogeneous nucleating reagent to promote the nucleation and growth of the pure PLLA. As expected, the thermal stability of OCPS/PLLA was improved due to the incorporation of inorganic cage. On the other hand, similar plasticizer effect of OCPS was also observed in the tensile test. The PLLA tensile behavior was changed from brittle to ductile by the incorporation of OCPS into PLLA matrix, and the strain at break was improved greatly.

## References

- Judeinstein, P.; Sanchez, C. *J Mater Chem* 1996, 6, 511.
- Pavlidou, S.; Papaspyrides, C. D. *Prog Polym Sci* 2008, 33, 1119.
- Spitalsky, Z.; Tasis, D.; Papagelis, K.; Galiotis, C. *Prog Polym Sci* 2010, 35, 357.
- Phillips, S. H.; Haddad, T. S.; Tomczak, S. J. *Curr Opin Solid State Mater Sci* 2004, 8, 21.
- Baney, R. H.; Itoh, M.; Sakakibara, A. *Chem Rev* 1995, 95, 1409.
- Voronkov, M. G.; Lavrent'ev, V. I. *Top Curr Chem* 1982, 102, 199.
- Kannan, R. Y.; Salacinski, H. J.; Butler, P. E.; Seifalian, A. M. *Acc Chem Res* 2005, 38, 879.
- Kopesky, E. T.; Haddad, T. S.; Cohen, R. E.; McKinley, G. H. *Macromolecules* 2004, 37, 8992.
- Zheng, L.; Farris, R. J.; Coughlin, E. B. *Macromolecules* 2001, 34, 8034.
- Xu, H. Y.; Kuo, S. W.; Lee, J. S.; Chang, F. C. *Macromolecules* 2002, 35, 8788.
- Lin, H.; Wu, S.; Huang, P.; Huang, C.; Kuo, S.; Chang, F. *Macromol Rapid Commun* 2008, 27, 1550.
- Kim, B.; Mather, P. *Macromolecules* 2006, 39, 9253.
- Choi, J.; Kim, S.; Laine, R. *Macromolecules* 2004, 37, 99.
- Hao, N.; Böning, M.; Goering, H.; Schöhal, A. *Macromolecules* 2007, 40, 2955.
- Ragauskas, A. J.; Williams, C. K.; Davison, B. H.; Britovsek, G.; Cairney, J.; Eckert, C. A.; Frederick, W. J., Jr.; Hallett, J. P.; Leak, D. J.; Liotta, C. L.; Mielenz, J. R.; Murphy, R.; Templer, R.; Tschaplinski, T. *Science* 2006, 311, 484.
- Cai, Q.; Wan, Y. Q.; Bei, J. Z.; Wang, S. G. *Biomaterials* 2003, 24, 3555.
- Auras, R.; Bruce, H.; Selke, S. *Macromol Biosci* 2004, 4, 835.
- Goffin, A.-L.; Duquesne, E.; Moins, S.; Alexandre, M.; Dubois, P. *Eur Polym J* 2007, 43, 4103.
- Lee, J. H.; Jeong, Y. G. *J Appl Polym Sci* 2009, 115, 1039.
- Wang, R.; Wang, S.; Zhang, Y. *J Appl Polym Sci* 2009, 113, 3095.
- Dittmar, U.; Hendan, B. J.; Florke, U.; Marsmann, H. C. *J. Organomet Chem* 1995, 489, 185.
- Liu, Y. H.; Yang, X. T.; Zhang, W. A.; Zheng, S. X. *Polymer* 2006, 47, 6814.
- Zhou, W. Y.; Duan, B.; Wang, M.; Cheung, W. L. *J Appl Polym Sci* 2009, 113, 4100.
- Sosnowski, S. *Polymer* 2001, 42, 637.
- Fischer, E. W.; Sterzel, H. J.; Wegner, G.; *Kolloid-Z.u.Z. Polymère* 1973, 251, 980.
- Feng, Y.; Jia, Y.; Xu, H. Y. *J Appl Polym Sci* 2009, 111, 2684.
- Chen, J. H.; Yao, B. X.; Su, W. B.; Yang, Y. B. *Polymer* 2007, 48, 1756.
- Soong, S. Y.; Cohen, R. E.; Boyce, M. C. *Polymer* 2007, 48, 1410.